> REPLACE THIS LINE WITH YOUR MANUSCRIPT ID NUMBER (DOUBLE-CLICK HERE TO EDIT) <

Suppression of optical fringes in gas spectroscopy inside anti-resonant hollow-core fibers by fiber bending

Grzegorz Gomółka, Patrycja Gronowicz, Adam Filipkowski, Ryszard Buczyński, and Michal Nikodem

Abstract—**Multimodal interference is frequently pointed out as one of the main limiting factors in gas sensing setups which utilize hollow-core optical fibers as gas cells. In this paper we demonstrate suppression of optical fringes that originate from propagation of higher order modes in an anti-resonant hollow-core fiber by controlled fiber bending. Near-infrared broadband absorption spectroscopy is used to characterize the fringe patterns observed when higher order modes are excited and suppressed. A tunable laser diode emitting near 1687 nm is used to present positive impact of bending the hollow-core fiber on signals recorded with both direct absorption spectroscopy and wavelength modulation spectroscopy of methane. Bending radius of 30 mm was found optimal for the setup presented in this work, leading to sub-ppm-level detection limit at 1687 nm with 7.35-m-long fiber.**

Index Terms—**anti-resonant hollow-core fiber, optical fringes suppression, laser gas spectroscopy, methane, near-infrared**

I. INTRODUCTION

HOLLOW-CORE fibers (HCFs) have been used in laser gas spectroscopy for approximately two decades, and many successful demonstrations in various spectral regions has been demonstrated [1], [2]. Hollow-core fiber

Grzegorz Gomółka and Michal Nikodem are with Department of Optics and Photonics, Wroclaw University of Science and Technology, 50-370 Wroclaw, Poland (e-mail: grzegorz.gomolka@pwr.edu.pl; michal.nikodem@pwr.edu.pl).

Patrycja Gronowicz is with Department of Optics and Photonics, Wroclaw University of Science and Technology, 50-370 Wroclaw, Poland, and also with Whitecarbon/Nanores, Bierutowska 57-59, 51-317 Wrocław, Poland (e-mail: patrycja.gronowicz@pwr.edu.pl).

Adam Filipkowski is with Department of Glass, Łukasiewicz Research Network - Institute of Microelectronics and Photonics, al. Lotników 32/46, 02-668 Warsaw, Poland (e-mail: adam.filipkowski@imif.lukasiewicz.gov.pl).

Ryszard Buczyński is with Faculty of Physics, University of Warsaw, Pasteura 5, 02-093 Warsaw, Poland, and also with Department of Glass, Łukasiewicz Research Network - Institute of Microelectronics and Photonics, al. Lotników 32/46, 02-668 Warsaw, Poland (e-mail: ryszard.buczynski@fuw.edu.pl).

family includes many different designs, such as hollow-core waveguides with inner reflective coatings, photonic bandgap hollow-core fibers (PBG-HCFs), Kagome hypocycloid lattice fibers or anti-resonant hollow-core fibers (AR-HCFs) [3]. Recently, the anti-resonant hollow-core fibers (often referred also as negative curvature fibers, NCFs) seem to attract the most attention in the field of gas sensing. Their main advantages include broad transmission windows that span even into mid-IR for silica-based fibers, low bending losses and large core diameter (which makes filling these fibers much faster than PBG-HCFs). They also typically have relatively simple tubular geometry, which makes them easier to design and manufacture than e.g. Kagome lattice HCFs. AR-HCFs have been applied to gas absorption spectroscopy using tunable semiconductor lasers to target numerous species, such as e.g. methane [4], [5], [6], ethane [7], nitrous oxide [8], [9], nitric oxide [10], carbon dioxide [11] or carbon monoxide [12] in both near- and mid-infrared. Other sensing techniques frequently used with AR-HCFs are photothermal spectroscopy [13], [14], [15] and chirped laser dispersion spectroscopy [16], [17]. Broadband absorption spectroscopy in photonic bandgap fibers had been explored in the past [18–20], but AR-HCFs have been used to assist broadband gas sensing techniques only very recently [18], [19].

When gas sensing is considered, the hollow-core fibers come with a range of advantages such as small footprint and mass, as well as ease of integration into all-fiber sensing setups with simplified, alignment-free design. On the other hand, fiber-based gas cells have some drawbacks, such as relatively long response time when HCFs longer than few meters are used [6], [7] or the presence of optical fringes from multimodal interference [4], [20], [21]. While the first issue does not affect directly the detection limit of the setup [22], the latter one is more problematic, as it directly affects measured signals. What is particularly troublesome, in many cases the interference fringes have periods close to the linewidths of the absorption lines being measured, so their filtration in post-processing is difficult or even impossible. While some gas sensing approaches use this interference to their advantage (e.g. mode-phase-difference photothermal spectroscopy [22]) for majority of methods the fringes significantly limit the performance of the sensor [23].

AR-HCFs can be designed to have large propagation loss for higher order modes (HOMs), which favors effectively single-mode propagation [24], [25], [26]. But even in well-designed fibers, higher order modes can be excited by non-

optimal light coupling. In some setups this was mitigated with the use of free-space mode-matching optical setups [8], [12], [27]. In all-fiber setups suppression of HOMs can be challenging, as the availability of integrated mode-matching microoptics is more limited [28], [29]. We have also observed that optical fringes can appear e.g. due to mechanical stress from fiber holders, even when proper coupling into HCF was provided, so development of other mode filtering methods is highly desired.

Recently, several studies have been published, in which the analysis of the impact of HCF bending on propagation losses of higher-order modes have been performed [30], [31], [32]. It has also been shown experimentally, that for the AR-HCFs, the energy from the core modes can be coupled to the cladding modes, if appropriate bending conditions are satisfied [33]. In this article we explore this phenomena with the aim to suppress the optical fringes from multimodal propagation inside the AR-HCF to enhance laser gas absorption spectroscopy. The first part of the paper presents numerical

simulations explaining the effects of bending the AR-HCF on light propagation. Subsequently, experimental results are shown and the application of bent HCF in absorption spectroscopy of methane in near-infrared is demonstrated.

II. ANALYTICAL AND NUMERICAL CALCULATIONS

The analytical formulas describing the bending effects on loss and modal purity of the light guided in a single-ring anti-resonant hollow core fiber were provided in ref. [32]. According to this work, critical values of bending radius R_{bc}^{pq} for LP_{pq}-like core modes, below which given core modes are strongly attenuated due to coupling to LP_{01} cladding tube modes, can be calculated for an idealized geometry of the AR-HCF from the following equation:

$$R_{bc}^{pq} = \frac{D^3}{\lambda^2} \frac{\pi^2 \left(1 + \frac{d}{D}\right)}{\left(u_{01}^2 \frac{D}{d}\right)^2 - u_{pq}^2} cos(\theta), \tag{1}$$
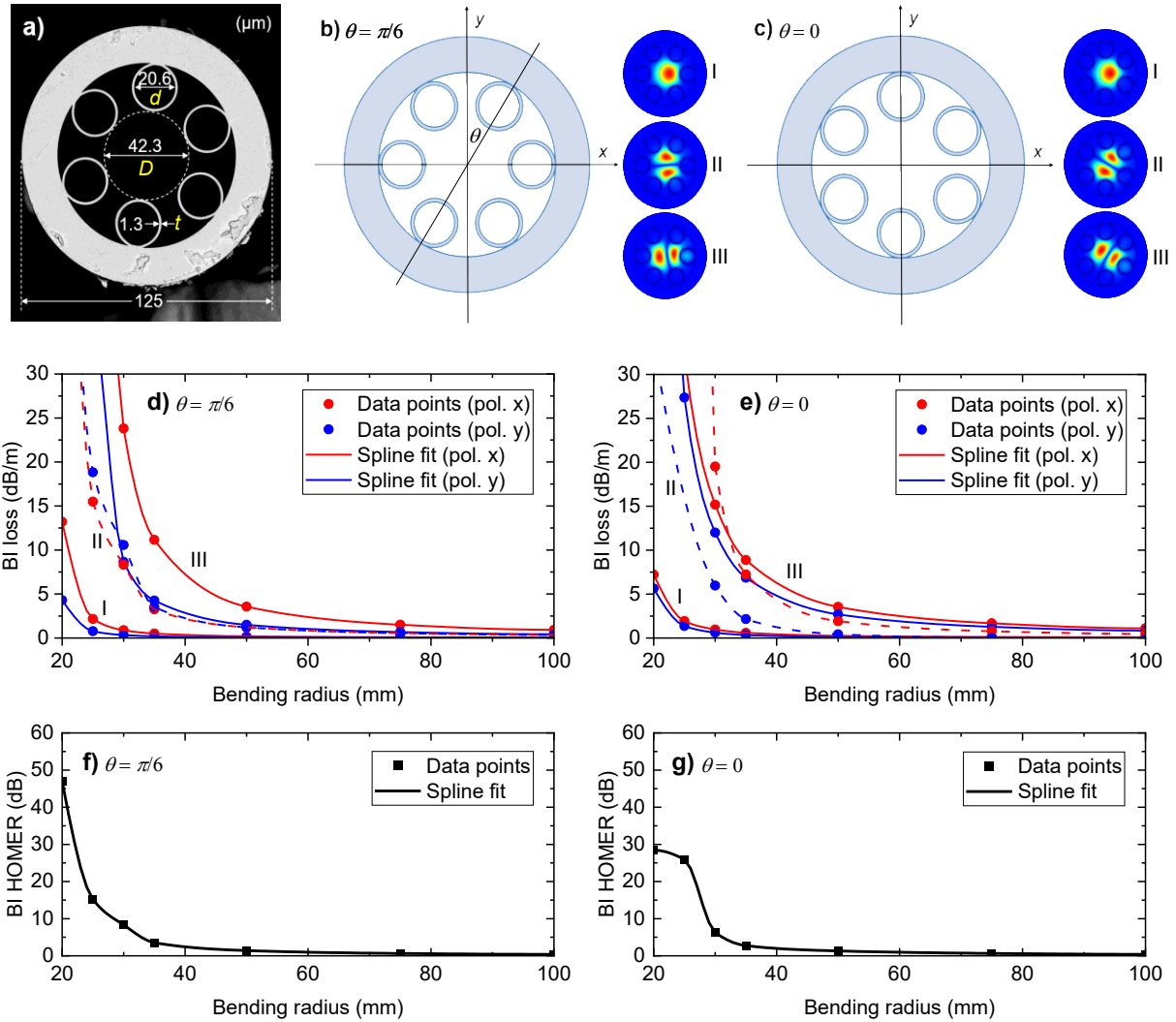

Fig. 1. (a) SEM image of the front facet of the AR-HCF used to obtain the geometry of the real fiber in COMSOL Multiphysics; **(b-c)** two simulated orientations of the AR-HCF with respect to the bending plane (*x*-axis) and spatial distributions of the electric field of these modes for bending radius of 50 mm for the two orientations; **(d-e)** bending induced loss of the first three modes of the AR-HCF for two orientations shown in (b-c), respectively; **(f-g)** bending induced HOMER of the AR-HCF for two orientations shown in (b-c), respectively.

where d and D are diameters of the cladding capillary and the core, respectively (see Fig. 1(a)), λ is the wavelength of light, u_{pq} is the q-th zero of the Bessel function J_p and θ is the rotation angle of the fiber equal to 0, when the centers of two cladding capillaries lie within y plane (see Fig. 1(b-c)). Using this equation allows to predict the tentative bending radius below which higher order modes should be effectively filtered. For instance, for LP$_{11}$-like modes the values of R_{bc}^{11} of 40.2 mm and 34.8 mm were obtained for θ of $\pi/6$ and 0, respectively. These values allows for rough estimation of the bending conditions at which the HOMs would be effectively suppressed.

In order to better understand the effect of bending of the actual AR-HCF used in experiments on suppression of higher order modes and obtain more precise estimations, the bending of the fiber was simulated numerically using finite elements method. The numerical model of the fiber was created with COMSOL Multiphysics 5.6 software. The real geometry of the six non-touching capillary silica AR-HCF was imported to the program using the high resolution (25 px/µm) SEM image of the fiber facet (see Fig. 1(a)). Bending of the fiber was simulated by application of the modified refractive index throughout the fiber domains (both air and silica) given by the formula:

$$n_b(x,y) = n(x,y)(1 + x/R_b), \qquad (2)$$

where R_b is the bending radius [34]. For a range of bending radii, the mode analysis was performed to find guided modes and obtain their attenuation constants in dB/m. From these values, bending induced loss (BI loss) of the guided modes, as well as bending induced higher order mode extinction ratio (BI HOMER) were calculated. These parameters have been previously introduced in [30] and are defined as the difference between the respective values for the fiber bent at R_b and the value for the straight fiber. Two series of simulations were performed for two orientations of the AR-HCF with respect to the bending plane (seen as x axis in Fig. 1(b-c)). Wavelength was set to 1.687 µm, as this was later used for experimental verification.

Decreasing the bending radius causes the change of the effective indices of the cladding modes and therefore facilitates the resonant coupling of the energy from core modes to the lossy modes propagating in the cladding capillaries or intercapillary spaces. The first modes to undergo this process are the higher order modes, so controlled bending can be used to provide effective modal filtering. Fig. 1(d-e) presents the BI losses of the first three modes found by the solver (marked I-III in the Fig. 1(b-c)). Even higher order modes were also found but their losses were much larger compared to the values obtained for modes II-III, so they were excluded from further analysis. Fig. 1(f-g) depicts the BI HOMER of the AR-HCF for two orientations. Both fiber orientations with respect to the bending plane yield similar efficiency of modal filtering. The area of increased BI HOMER (over ~10 dB) was obtained for bending radius of ~28.5 mm. This prediction based on the numerical study turned out to be in very good agreement with the experimental results presented in Section III.

III. Experimental results

Because AR-HCF pieces used in this study were few meters long, for practical reasons they have to be coiled into loops. With bending radius greater than 100 mm we did not observe any significant bending losses, nor any visible improvement related to higher order mode suppression. Therefore, within this manuscript this state will be consequently called 'unbent' HCF. Actual bending of the fiber was performed by attaching the coiled fiber to the side surface of the Styrofoam cone, as schematically shown in Fig. 2(a). Bend radii from 50 mm down to 17.5 mm could be used.

A. Broadband spectroscopy of methane in bent AR-HCF

The optical fringes from higher order mode interference were observed in a broad wavelength range in the setup presented in Fig. 2(a). We used a home-made supercontinuum (SC) source and optical spectrum analyzer (from Yokogawa, model AQ6370B). The light from the SC was coupled to the 4.3-m-long AR-HCF with a standard single mode fiber with FC-APC connector (to minimize the reflections). The HCF ends were terminated with temporary fiber connectors (from Thorlabs, models BFT1 & B30126C3). A modified mating sleeve with two drilled side channels and rubber O-rings was used to enable filling the HCF with gas mixtures. The HCF itself was coiled (7 loops) onto the Styrofoam cone described earlier. Fig. 2(b) presents the measured attenuation spectrum of the hollow-core fiber that indicates a transmission band that spans from ~1450 nm to ~1970 nm.

In order to characterize the impact of bending the AR-HCF on the magnitude of the optical fringes, we performed a series of acquisitions for two spectral windows near 1651 and 1687 nm (both windows can be used to measure absorption lines of methane). During these measurements, the HCF was
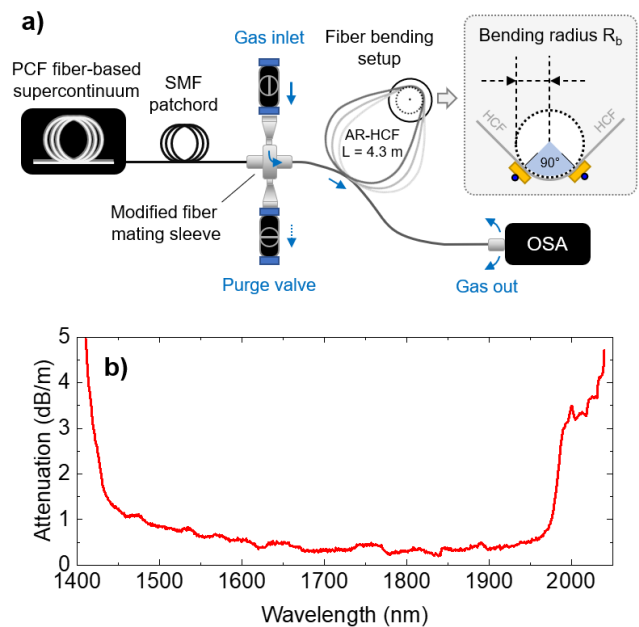

Fig.2. **(a)** The experimental setup used for demonstration of broadband methane spectroscopy inside bent AR-HCF and the schematic explaining the method of HCF bending on the Styrofoam cone; **(b)** measured attenuation of the AR-HCF.
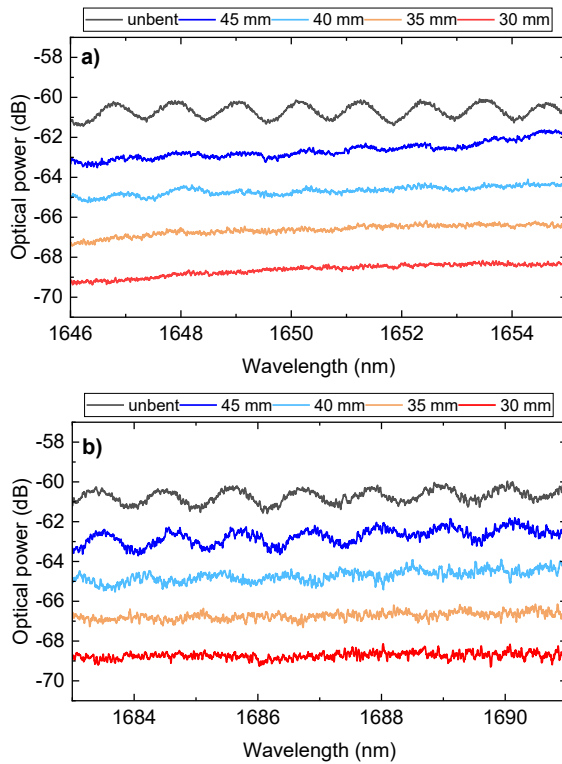
Fig.3. Interference fringes observed in the nitrogen-filled AR-HCF in the vicinity of 1651 nm **(a)** and 1687 nm **(b)** (vertical offsets were added for clarity).

filled with pure nitrogen (so there are no absorption lines of methane or any other gas in Fig. 3). Spectra demonstrated in Fig. 3 have been recorded for unbent HCF and for four decreasing bending radii (45, 40, 35 and 30 mm). Vertical offsets in Fig. 3 were added in order to show all five spectra clearly. It can be noticed that optical fringes can be efficiently suppressed for bending radii smaller than ~35 mm. This is in a very good agreement with the predictions from numerical simulations presented in Section II. By comparison of traces for 1651 nm and 1687 nm, it is also visible, that for shorter wavelength effective suppression of fringes is achieved for larger bending radius, as the critical value of bending radius R_{bc}^{pq} is proportional to $1/\lambda^2$, as presented in equation (1).

Fig. 4(a-b). demonstrates optical spectra of AR-HCF filled with pure N_2 and 1.8% CH_4 in synthetic air (20.9% O_2 balanced with N_2), both at atmospheric pressure, in two scenarios: when the fiber was not bent (a) and when it was bent with radius of 30 mm (b). From Fig. 4(a-b) it is clear that bending the AR-HCF during measurement significantly reduces the optical fringes, enabling more efficient reconstruction of the baseline. As shown in Fig. 4(c) the measurement agrees very well with the simulation based on HITRAN database.
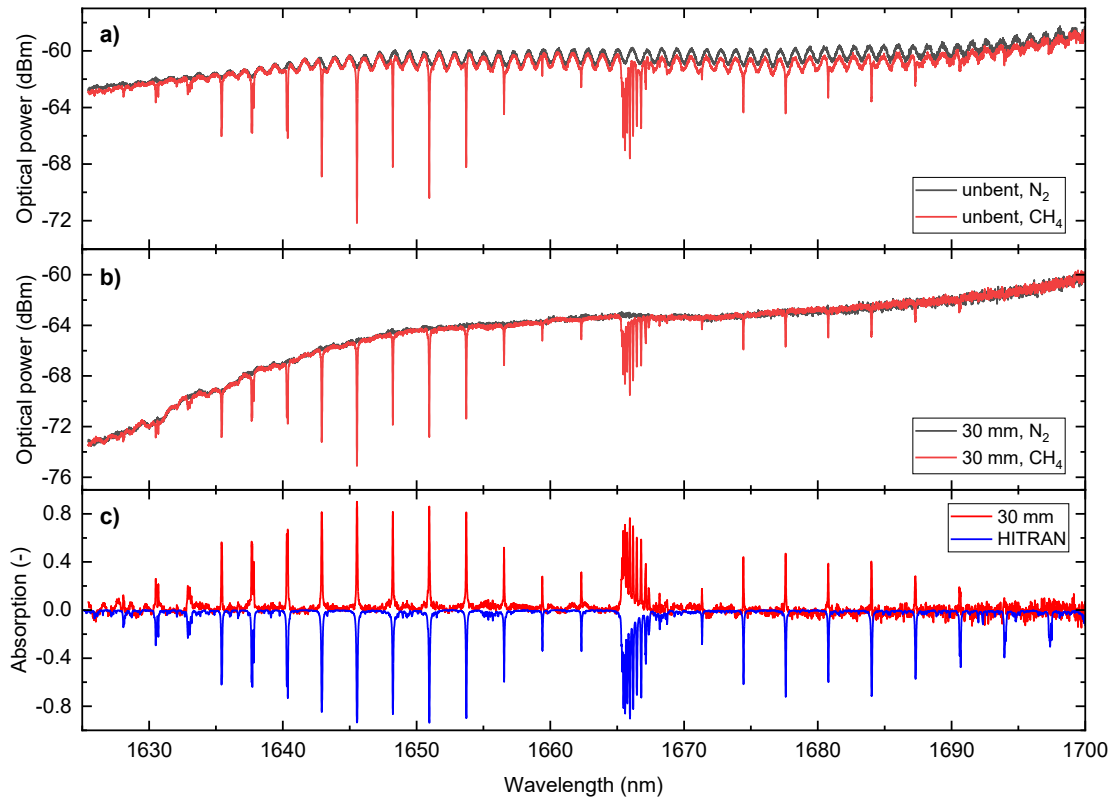

Fig. 4. Transmission spectra of the unbent **(a)** and bent at R_b = 30 mm **(b)** AR-HCF filled with N_2 and 1.8% CH_4; **(c)** methane absorption spectrum in near-IR obtained in bent AR-HCF compared with HITRAN database.

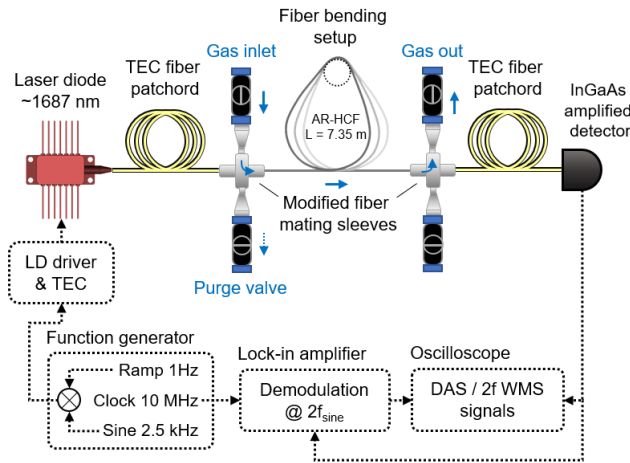## B. Tunable laser diode spectroscopy of methane inside bent AR-HCF

Fig.5. The experimental setup used for tunable laser diode methane spectroscopy inside bent AR-HCF (note: for direct absorption spectroscopy the sine modulation and lock-in amplifier were disabled).

The suppression of the optical interference fringes in AR-HCFs is particularly important in gas detection/spectroscopy with tunable laser diodes (TDLAS). With optical fringes observed typically in HCF-based setups, the tuning range of laser diodes usually allows to record only small part of the fringe pattern, making it hard to distinguish between optical fringe baseline and molecular absorption line. To demonstrate
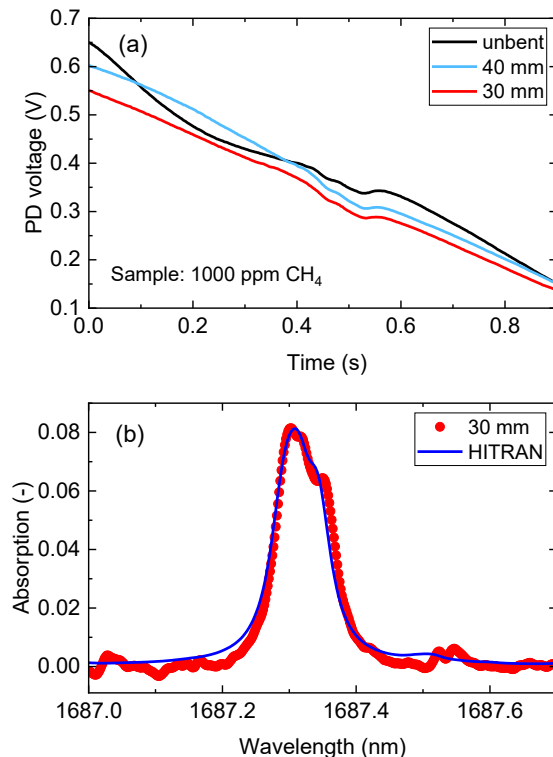

Fig.6. (a) Direct absorption spectroscopy scans for three AR-HCF bending conditions recorded when the LD wavelength was tuned across the CH_4 line near 1687 nm; **(b)** absorption spectra retrieved from DAS scans (simulation based on HITRAN).

fringe suppression in practical sensing system, a measurement setup shown in Fig. 5 was built. The setup comprises the discrete-mode laser diode emitting near 1687 nm (Eblana Photonics, model EP1687-3-DM-B06-FA), where an absorption feature of CH_4 is located (as shown in Fig. 6(a-b)). For initial measurements, 1000 ppm CH_4 sample was used. The light from the laser diode was coupled into the 7.35-m-long piece of the AR-HCF through thermally-expanded-core (TEC) single mode patch cable (from Thorlabs, model P5-1550TEC-2) for better matching the mode field areas of the fibers (~19 µm for TEC SMF and ~38 µm for AR-HCF). With this approach, the insertion loss was typically below 3 dB. The two fibers were connected in the modified mating sleeve with side channels which allowed for filling the core of the AR-HCF with gas sample. When the AR-HCF was coiled onto the Styrofoam cone, 12 loops were used. The light from the HCF was collected by the second TEC patch cable in the second mating sleeve and guided to the amplified InGaAs photodetector (Thorlabs, mod. PDA10CS2). The lock-in amplifier (Zurich Instruments, model UHFLI) was used to retrieve the second harmonic signal (2f WMS signal) in wavelength modulation spectroscopy experiments.

Direct absorption spectroscopy (DAS) scan presented in Fig. 6(a) for unbent HCF clearly indicate the presence of interference fringes. Because the background of the signal is complex and changes dynamically with time and measurement conditions, in practice it is not possible to measure the baseline (using nitrogen as sample). It would also be very challenging to correctly and reliably retrieve the baseline by fitting it with polynomial. In that case suppressing higher-order modes becomes essential. Fig. 6(b) shows absorption spectrum of 1000 ppm CH_4 with removed baseline, when the HCF was bent with radius of 30 mm, together with spectrum simulated using HITRAN database. Good agreement between the simulation and measurement in bent fiber is obtained. The absorption spectra calculated from scans in unbent fiber could also be obtained, but the line shapes were inconsistent with each other due to dynamically changing background.

Fringes are also present in the second harmonic WMS signals. As shown in Fig. 7(a), optical fringes could be effectively suppressed when bending radius smaller or equal to 30 mm was used, which corresponds well with the earlier observations from broadband measurements (Section II). It is worth mentioning that with the decrease of the bending radius R_b, the transmitted optical power drops, so once the higher-order modes are successfully suppressed, further bending of the HCF is not recommended. For instance, no significant/visible background improvement is observed in 2f WMS spectra in Fig. 7(a) for bending radius of 25 mm, compared to 30 mm, but the amplitude of the 2f WSM signal decreases due to drop of optical power.

Bent fiber was also used to perform WMS with smaller methane concentrations of 100 ppm and 23.9 ppm, both mixed with synthetic air. The spectra measured in bent AR-HCF (R_b = 30 mm) are shown in Fig. 7(b). The backgrounds of recorded 2f WMS signals are free from any optical fringes.
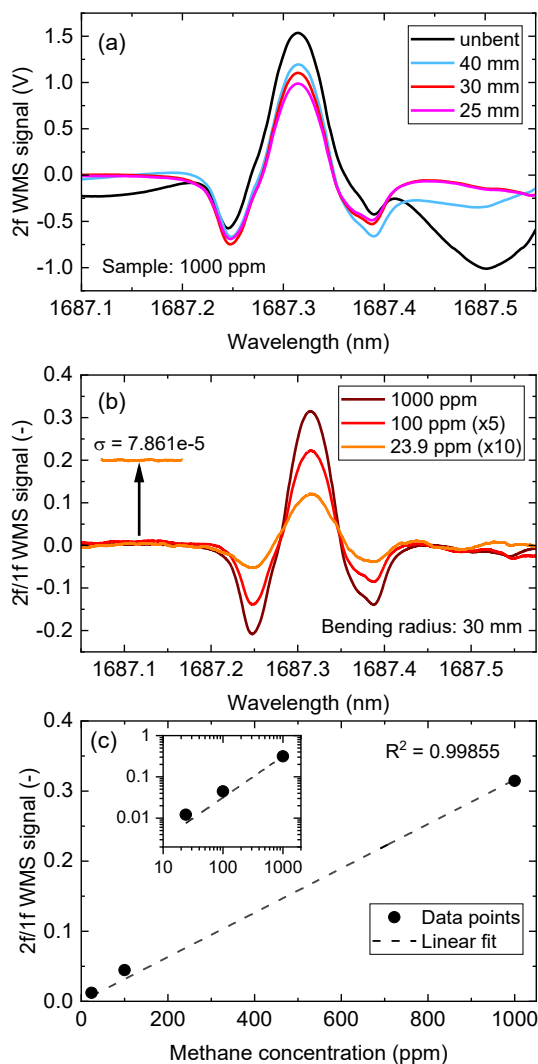
Fig.7. (a) 2f WMS spectra for four bending conditions; **(b)** 2f/1f WMS spectra for three CH_4 concentrations recorded when the fiber bending radius was 30 mm; **(c)** Linear fit of the peak value of 2f/1f WMS dependency on the methane concentration inside AR-HCF.

The deviation from zero for longer wavelengths, i.e. 1687.45 nm and above, is related to the spectroscopic properties of the CH_4 line in this spectral region and also tuning properties of the laser diode. To present signals for various concentrations in one graph they had to be magnified (Fig. 7(b)), which also required the wings of the 2f WMS signal to be corrected using a 3rd order polynomial. Signal normalization to 1f WMS was also applied. Based on the standard deviation of the 2f/1f WMS signal away from the absorption line, the detection limit of the sensor was estimated to be 0.155 ppm CH_4 (for the signal-to-noise ratio equal to 1 for the signal measured with the HCF filled with the sample of 23.9 ppm CH_4).

IV. DISCUSSION

In this paper we present a simple and efficient method of HOM interference suppression by controlled bending of the anti-resonant hollow-core fiber. The method is backed up by the analytical and numerical mode analysis of the used six non-touching capillary AR-HCF for the range of the bending

radii. With calculations we were able to identify radii values for which increased bending induced loss and BI HOMER are expected. Numerically obtained behavior exhibits exceptional agreement with the experimental observations.

The approach was demonstrated in two gas sensing methods, i.e. broadband absorption spectroscopy using supercontinuum source and narrowband absorption spectroscopy using tunable laser diode. In both techniques, efficient filtration of the HOMs was presented by the fiber bending and the optical fringes coming from their interference were marginalized. The suppression of optical fringe allows for efficient baseline correction in direct absorption spectroscopy, either by N_2 background measurement or fitting.

Fiber bending increases the loss of all modes propagating in HCF, so it is important to select the right bending radius, which will enable efficient HOM suppression but maintain overall optical loss at acceptable level. Analytical solutions presented in [32] can be used to get a rough estimate of the critical bending radius, which will be a good starting point for the experiments. It is also worth noting, that this value is wavelength dependent, so in case of broadband spectroscopy, the longest wavelength should be considered. In the case of AR-HCF used in this work and for wavelength of 1687 nm the optimal value of bending radius was determined to be 30 mm. For this radius, the calculated BI loss of the HOMs was of the order of tens of dB/m (depending on the order of the HOM), while the BI loss of the fundamental mode was at the level of few dB/m. The measured optical loss at 1687 nm in TDLAS experiments was 2.1 dB/m at bending radius of 30 mm, what stays in good agreement with numerical simulation. It was therefore presented, that both analytical and numerical estimations of AR-HCF bending effects can become valuable tools in spectroscopic systems design.

Overall, the presented approach of HOM suppression to enhance laser gas spectroscopy is simple, robust, and versatile, what allows it to be easily applied in many sensing schemes and techniques that use AR-HCFs as the gas cells. Of course, not all HCFs allow for efficient filtration of HOMs by bending (some fibers have large sensitivity to bending by design) or are deliberately designed to guide multiple modes. Still, in many cases, the presented technique can yield a significant improvement in the performance of the sensor at no additional cost.

V. CONCLUSIONS

In this work we reported an effective method of suppression of optical fringes from higher order mode propagating inside AR-HCFs. The suppression was obtained by the controlled bending of the fiber. Phenomenon of modal filtration was investigated analytically and with numerical simulations in COMSOL Multiphysics environment. Simulations and experimental results are in very good agreement. Both broadband and narrowband spectral measurements in near-infrared were demonstrated, using methane as target gas. For the HCF used in this work, bending radius of 30 mm was found optimal for gas sensing free from HOM interference fringe background. Methane sensing inside 7.35-m-long HCF using wavelength modulation spectroscopy was demonstrated with the detection limit of 0.155 ppm.

This article has been accepted for publication in IEEE Journal of Selected Topics in Quantum Electronics. This is the author's version which has not been fully edited and content may change prior to final publication. Citation information: DOI 10.1109/JSTQE.2024.3367272

7

> REPLACE THIS LINE WITH YOUR MANUSCRIPT ID NUMBER (DOUBLE-CLICK HERE TO EDIT) <

REFERENCES

[1] W. Jin et al., "Recent Advances in Spectroscopic Gas Sensing With Micro/Nano-Structured Optical Fibers," *Photonic Sensors*, vol. 11, no. 2, pp. 141–157, Jun. 2021, doi: 10.1007/s13320-021-0627-4.

[2] P. Jaworski, "A review of antiresonant hollow-core fiber-assisted spectroscopy of gases," *Sensors*, vol. 21, no. 16. MDPI AG, Aug. 02, 2021. doi: 10.3390/s21165640.

[3] B. Debord, F. Amrani, L. Vincetti, F. Gérôme, and F. Benabid, "Hollow-core fiber technology: The rising of 'gas photonics,'" *Fibers*, vol. 7, no. 2. MDPI Multidisciplinary Digital Publishing Institute, pp. 1–58, 2019. doi: 10.3390/FIB7020016.

[4] J. Kapit and A. P. M. Michel, "Dissolved gas sensing using an anti-resonant hollow core optical fiber," *Appl Opt*, vol. 60, no. 33, pp. 10354–10358, Nov. 2021, doi: 10.1364/ao.439787.

[5] P. Jaworski et al., "Antiresonant hollow-core fiber-based dual gas sensor for detection of methane and carbon dioxide in the near-and mid-infrared regions," *Sensors*, vol. 20, no. 14, pp. 1–12, Jul. 2020, doi: 10.3390/s20143813.

[6] G. Gomółka, G. Stępniewski, D. Pysz, R. Buczyński, M. Klimczak, and M. Nikodem, "Highly sensitive methane detection using a mid-infrared interband cascade laser and an anti-resonant hollow-core fiber," *Opt Express*, vol. 31, no. 3, pp. 3685–3697, Jan. 2023, doi: 10.1364/oe.479963.

[7] P. Jaworski et al., "Sub parts-per-billion detection of ethane in a 30-meters long mid-IR Antiresonant Hollow-Core Fiber," *Opt Laser Technol*, vol. 147, p. 107638, Mar. 2022, doi: 10.1016/j.optlastec.2021.107638.

[8] C. Yao, S. Gao, Y. Wang, P. Wang, W. Jin, and W. Ren, "Silica Hollow-Core Negative Curvature Fibers Enable Ultrasensitive Mid-Infrared Absorption Spectroscopy," *Journal of Lightwave Technology*, vol. 38, no. 7, pp. 2067–2072, Apr. 2020, doi: 10.1109/JLT.2019.2960804.

[9] M. Nikodem, G. Gomółka, M. Klimczak, D. Pysz, and R. Buczyński, "Demonstration of mid-infrared gas sensing using an anti-resonant hollow core fiber and a quantum cascade laser," *Opt Express*, vol. 27, no. 25, pp. 36350–36357, Dec. 2019, doi: 10.1364/oe.27.036350.

[10] K. Krzempek, P. Jaworski, P. Kozioł, and W. Belardi, "Antiresonant hollow core fiber-assisted photothermal spectroscopy of nitric oxide at 5.26 μm with parts-per-billion sensitivity," *Sens Actuators B Chem*, vol. 345, p. 130374, Oct. 2021, doi: 10.1016/j.snb.2021.130374.

[11] M. Nikodem, G. Gomółka, M. Klimczak, D. Pysz, and R. Buczyński, "Laser absorption spectroscopy at 2 μm inside revolver-type anti-resonant hollow core fiber," *Opt Express*, vol. 27, no. 10, pp. 14998–15006, May 2019, doi: 10.1364/oe.27.014998.

[12] C. Yao et al., "Sub-ppm CO detection in a sub-meter-long hollow-core negative curvature fiber using absorption spectroscopy at 2.3 μm," *Sens Actuators B Chem*, vol. 303, p. 127238, Jan. 2020, doi: 10.1016/j.snb.2019.127238.

[13] P. Zhao, H. L. Ho, W. Jin, S. Fan, S. Gao, and Y. Wang, "Hollow-core fiber photothermal methane sensor with temperature compensation," *Opt Lett*, vol. 46, no. 11, pp. 2762–2765, Jun. 2021, doi: 10.1364/ol.426812.

[14] K. Krzempek, P. Jaworski, P. Kozioł, and W. Belardi, "Antiresonant hollow core fiber-assisted photothermal spectroscopy of nitric oxide at 5.26 μm with parts-per-billion sensitivity," *Sens Actuators B Chem*, vol. 345, p. 130374, Oct. 2021, doi: 10.1016/j.snb.2021.130374.

[15] C. Yao, S. Gao, Y. Wang, W. Jin, and W. Ren, "Heterodyne interferometric photothermal spectroscopy for gas detection in a hollow-core fiber," *Sens Actuators B Chem*, vol. 346, p. 130528, Nov. 2021, doi: 10.1016/j.snb.2021.130528.

[16] P. Jaworski, K. Krzempek, P. Bojęś, D. Wu, and F. Yu, "Mid-IR antiresonant hollow-core fiber based chirped laser dispersion spectroscopy of ethane with parts per trillion sensitivity," *Opt Laser Technol*, vol. 156, p. 108539, Dec. 2022, doi: 10.1016/j.optlastec.2022.108539.

[17] M. Hu, A. Ventura, J. G. Hayashi, F. Poletti, S. Yao, and W. Ren, "Trace gas detection in a hollow-core antiresonant fiber with heterodyne phase-sensitive dispersion spectroscopy," *Sens Actuators B Chem*, vol. 363, p. 131774, Jul. 2022, doi: 10.1016/j.snb.2022.131774.

[18] Q. Wang et al., "Dual-comb photothermal spectroscopy," *Nat Commun*, vol. 13, no. 1, p. 2181, Dec. 2022, doi: 10.1038/s41467-022-29865-6.

[19] K. Johnson et al., "Hollow-core fiber delivery of broadband mid-infrared light for remote spectroscopy," *Opt Express*, vol. 30, no. 5, pp. 7044–7052, Feb. 2022, doi: 10.1364/oe.450413.

[20] F. Yang, W. Jin, Y. Cao, H. L. Ho, and Y. Wang, "Towards high sensitivity gas detection with hollow-core photonic bandgap fibers," *Opt Express*, vol. 22, no. 20, pp. 24894–24907, Oct. 2014, doi: 10.1364/oe.22.024894.

[21] J. P. Parry et al., "Towards practical gas sensing with micro-structured fibres," *Meas Sci Technol*, vol. 20, no. 7, p. 075301, 2009, doi: 10.1088/0957-0233/20/7/075301.

[22] P. Zhao et al., "Mode-phase-difference photothermal spectroscopy for gas detection with an anti-resonant hollow-core optical fiber," *Nat Commun*, vol. 11, no. 1, p. 847, Dec. 2020, doi: 10.1038/s41467-020-14707-0.

[23] P. Werle, "Accuracy and precision of laser spectrometers for trace gas sensing in the presence of optical fringes and atmospheric turbulence," *Appl Phys B*, vol. 102, no. 2, pp. 313–329, Feb. 2011, doi: 10.1007/s00340-010-4165-9.

[24] A. Ge, F. Meng, Y. Li, B. Liu, and M. Hu, "Higher-order mode suppression in antiresonant nodeless hollow-core fibers," *Micromachines (Basel)*, vol. 10, no. 2, pp. 1–12, Feb. 2019, doi: 10.3390/mi10020128.

[25] Z. Chen, P. Jiang, W. Caiyang, F. Gui, M. Wang, and H. Yang, "Higher-order modes suppression in negative curvature anti-resonance hollow core fibers by multiple resonant coupling," *Opt Commun*, vol. 475, p. 126246, Nov. 2020, doi: 10.1016/j.optcom.2020.126246.

[26] P. Uebel et al., "Broadband robustly single-mode hollow-core PCF by resonant filtering of higher-order modes," *Opt Lett*, vol. 41, no. 9, pp. 1961–1964, May 2016, doi: 10.1364/ol.41.001961.

[27] L. Hu et al., "A hollow-core photonic band-gap fiber based methane sensor system capable of reduced mode interference noise," *Infrared Phys Technol*, vol. 97, pp. 101–107, Mar. 2019, doi: 10.1016/j.infrared.2018.12.023.

[28] Y. Jung et al., "Compact micro-optic based components for hollow core fibers," *Opt Express*, vol. 28, no. 2, pp. 1518–1525, Jan. 2020, doi: 10.1364/oe.28.001518.

[29] D. Suslov et al., "Low loss and high performance interconnection between standard single-mode fiber and antiresonant hollow-core fiber," *Sci Rep*, vol. 11, no. 1, p. 8799, Dec. 2021, doi: 10.1038/s41598-021-88065-2.

[30] Y. Wang and W. Chang, "Understanding bending-induced loss and bending-enhanced higher-order mode suppression in negative curvature fibers," *Opt Express*, vol. 29, no. 15, pp. 23622–23636, Jul. 2021, doi: 10.1364/oe.432314.

[31] R. M. Carter et al., "Measurement of resonant bend loss in anti-resonant hollow core optical fiber," *Opt Express*, vol. 25, no. 17, pp. 20612–20621, Aug. 2017, doi: 10.1364/oe.25.020612.

[32] M. H. Frosz, P. Roth, M. C. Günendi, and P. St. J. Russell, "Analytical formulation for the bend loss in single-ring hollow-core photonic crystal fibers," *Photonics Res*, vol. 5, no. 2, p. 88, Apr. 2017, doi: 10.1364/prj.5.000088.

[33] G. K. Alagashev, A. D. Pryamikov, A. F. Kosolapov, A. N. Kolyadin, A. Y. Lukovkin, and A. S. Biriukov, "Impact of geometrical parameters on optical properties of negative curvature hollow-core fibers," *Laser Phys*, vol. 25, no. 5, p. 055101, 2015, doi: 10.1088/1054-660X/25/5/055101.

[34] R. T. Schermer and J. H. Cole, "Improved bend loss formula verified for optical fiber by simulation and experiment," *IEEE J Quantum Electron*, vol. 43, no. 10, pp. 899–909, 2007, doi: 10.1109/JQE.2007.903364.

Grzegorz Gomółka received the B.Sc. degree in biomedical optics in 2019, and the M.Sc. degree in optics and photonics in 2020. He is currently working toward the graduation degree with the Department of Optics and Photonics, Wrocław University of Science and Technology, Wrocław, Poland. His research interests include applications of hollow-core optical fibers in gas absorption sensors and novel methods and configurations in laser spectroscopy.

Patrycja Gronowicz received the B.Sc degree in material engineering in 2020, and the M.Sc degree in mechanical engineering, specialty of construction materials engineering in 2021. She is currently working toward the PhD at the Department of Optics and Photonics, Wrocław University of Science and Technology, Wrocław, Poland. Her research interests include preparation, analysis and modifications of conductive and non-conductive materials using SEM/FIB electron microscopes.

Adam Filipkowski received his MSc degree in physics from the University of Warsaw. His PhD degree in physics was awarded by the Heriot-Watt University, Edinburgh, U.K. in 2016. He is currently an Assistant Professor at Faculty of Physics, University of Warsaw and also holds a position at Łukasiewicz Institute of Microelectronics and Photonics in Warsaw. His research interests include photonic crystal fibers, nanostructured GRIN optical elements, and specialty fibers which integrated glasses and metals.

Ryszard Buczyński received the M.Sc. and Ph.D. degrees in physics from the Warsaw University of Technology, Warsaw, Poland, in 1994 and 1999, respectively, and the second Ph.D. degree in applied science from Vrije Universiteit Brussel, Brussel, Belgium, in 2000. During his academic career, he was a Postdoctoral Fellow with Vrije Universiteit Brussel and with Heriot-Watt University, Edinburgh, U.K. He is currently a Professor with the Institute of Microelectronics and Photonics, Warsaw, and with the Faculty of Physics, University of Warsaw, Warsaw. He leads an interuniversity research team Microoptics and Photonic Crystal Fibers Group. He has coauthored more than 100 publications in peer-reviewed journals. His research interests include photonic crystal fibers, supercontinuum generation, microoptics, microfluidics, and development of nonlinear photonic crystal fibers based on soft glasses and nanostructured micro optical components.

Michal Nikodem received the Ph.D. degree from the Wrocław University of Technology, Wrocław, Poland, in 2010. After postdoctoral fellowship with Princeton University, Princeton, NJ, USA, during 2010–2012, he joined Wrocław Research Centre EIT+, where he has been working on spectroscopic systems for chemical analysis. In 2017, he was appointed by the Department of Optics and Photonics, Wrocław University of Science and Technology, Wrocław. His research interests include laser-based sensing, mid- and near-infrared spectroscopy, and novel optical fibers.